

②
B.S.

LEVEL II

ESD-TR-80-84

AD A 088332

THE EVALUATION OF MODELS FOR ATMOSPHERIC
ATTENUATION AND BACKSCATTER CHARACTERISTIC ESTIMATION
AT 95 GHZ

February 1978

ERT Document No. P-3606

See 11173

Prepared for

MIT Lincoln Laboratory
Purchase Order AX 14398
Prime Contract F19628-78-C-0002

S DTIC ELECTE D
AUG 22 1980
B

Prepared by

Robert K. Crane and Hsiao-hua K. Burke
Environmental Research & Technology, Inc.
696 Virginia Road
Concord, Massachusetts 01742

Approved for public release; distribution unlimited.

JDC FILE COPY

80 8 22 012

The views and conclusions contained in this document are those of the contractor and should not be interpreted as necessarily representing the official policies, either expressed or implied, of the United States Government.

This technical report has been reviewed and is approved for publication.

FOR THE COMMANDER

Raymond L. Loiselle

Raymond L. Loiselle, Lt. Col., USAF
Chief, ESD Lincoln Laboratory Project Office

1. INTRODUCTION

Active or passive observations of targets on the surface of the earth at a frequency of 95 GHz may be adversely affected by the presence of rain or cloud along the observation path, in the vicinity of the target, or above the target. The effects of rain or cloud on system performance may be simulated given the characteristics of the system and models for attenuation and scattering by the rain or cloud particles. The validity of the simulation results depends upon the veracity of the rain or cloud model. In this brief report, models for attenuation and scattering by rain are reviewed and compared with experimental observations. Models for the calculation of attenuation due to clouds and the clear atmosphere are also presented.

Calculations of the scattering properties of rain drops have been made many times over the past four decades. The results of these calculations have been used to model attenuation effects for radar and communication systems and to calibrate weather radar systems for use in measuring rainfall. The adequacy of the calculations for the estimation of attenuation over a wide frequency range has received considerable attention. Medhurst (1965) reviewed the results of experiments made prior to 1964 and concluded that the measurements and theory did not agree. He suggested that a purely empirical approach should be used for the estimation of specific attenuation at a given rain rate. deBettencourt (1974) also reviewed the state of the experimental observations made prior to 1972 and concluded that an empirical procedure should be used for the estimation of specific attenuation although he could not find conclusive evidence that the theory and observations disagreed. Crane (1971, 1975) and Waldteufel (1973) reviewed the available data and reached the conclusion that theory and observation do agree and that the theoretical relationship between specific attenuation and rain rate should be used; they found that the difficulties lay in the problems of measuring the rainfall intensity along a path. Crane (1974) in a carefully controlled experiment showed that good agreement existed between measurements and theory. Joss et al (1974) reached a similar conclusion after careful analysis of another experiment. Today, the adequacy of model computations for the estimation of specific attenuation for a given rainfall rate is generally accepted for frequencies below 40 GHz.

A similar situation exists for the estimation of the backscatter cross section per unit volume (reflectivity) for a given rain rate. At frequencies below 10 GHz, the adequacy of the theory for the calculation of reflectivity is well established. Uncertainties in the relationship between reflectivity and rain rate are due primarily to uncertainties in the drop size distribution that should be used for the rain filled volume. Secondary problems exist associated with the drop shape distribution to be used but the corrections for shape are generally less than 2 dB. Crane and Glover (1978) recently reviewed the calibration procedures for the SPANDAR S-band radar at Wallops Island, Virginia and found that with a good radar calibration procedure, a detailed knowledge of the drop size distribution and corrections for drop shape, radar observations and cross section estimates based on rain rate observations agree to within 0.9 dB rms. The uncertainty in the comparison was primarily associated with difficulties in estimating the rain rate for comparison with the radar measurements.

Thus, it is concluded that models for the estimation of rain effects are well established for use at frequencies below 40 GHz. At higher frequencies the possibility of uncertainties still exist. The uncertainties are primarily associated with the distribution of rain and cloud particles in the region of interest and are not associated with theoretical problems.

ACCESS ON for	
NTIS	White Section <input checked="" type="checkbox"/>
DDC	Buff Section <input type="checkbox"/>
UNANNOUNCED	<input type="checkbox"/>
JUSTIFICATION	
BY	
DISTRIBUTION/AVAILABILITY CODES	
Dist.	A.A.C. and/or SPECIAL
A	

2. ATTENUATION AND SCATTERING BY RAIN AT FREQUENCIES ABOVE 20 GHZ

2.1 Attenuation

Model calculations for specific attenuation and reflectivity have been available for many years. Crane (1966) made a series of calculations using the standard assumptions: spherical rain drops with homogeneous dielectric properties distributed in space in accordance with a Poisson process. He reported the results of calculations made for 35, 70, and 94 GHz using both a model drop size distribution and a number of measured distributions. More recently, Crane (1977) published an analysis of the sampling errors associated with drop size measurements which showed that a significant fraction of the spread of the calculations for individual drop size distributions about calculations based on the use of the Laws and Parsons distributions (Laws and Parsons, 1943) was caused by sampling effects.

Calculations of specific attenuation and of the backscatter cross section per unit volume are presented in Figures 1 and 2 respectively, for two model distributions, the Laws and Parsons (L&P) distributions (Laws and Parsons, 1943) and the Marshall-Palmer (M-P) distribution (Marshall and Palmer, 1948). The essential difference between the two distributions is in the number of small drops, the M-P distribution containing significantly more small drops than L&P. The results of the calculations show that the number of small drops can seriously affect the estimate of attenuation at frequencies above 30 GHz and rain rates above 10 mm/h.

The summary of observations compiled by deBettencourt (1974) shows good agreement between the theoretical estimates and observations when the observations are culled to remove (1) observations made prior to 1950, (2) observations made with a large separation between the measurement path and the rain gauges, and (3) observations with known difficulties in the interpretation of the rain gauge data. The summary figure from deBettencourt is reproduced in Figure 3 together with the recent published measurements of Sander (1975). The questionable data are marked by (X), the acceptable data by (●). The theoretical power law curve was based on a regression of a large number of calculations based

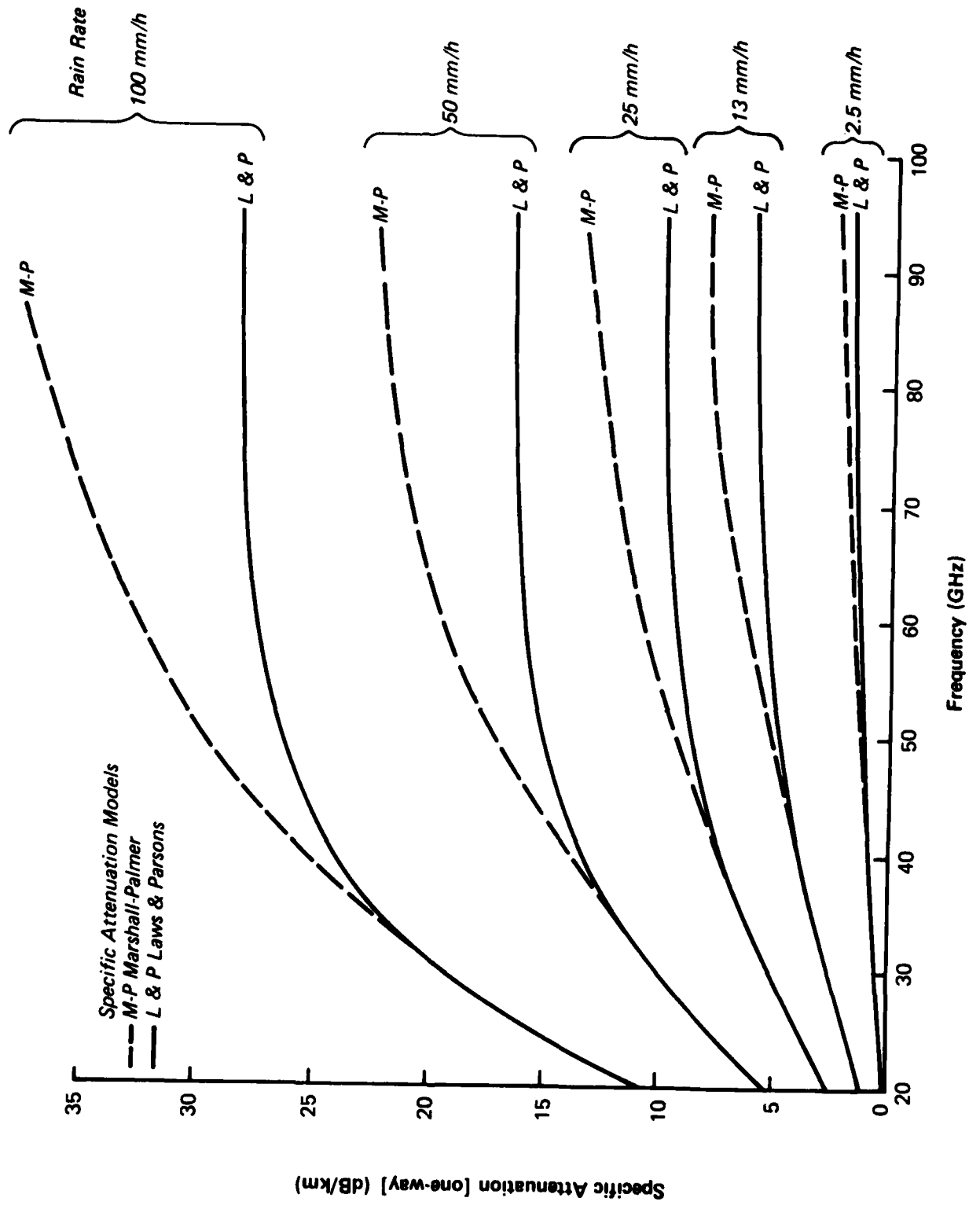


Figure 1 One Way Specific Attenuation vs Frequency for Rain

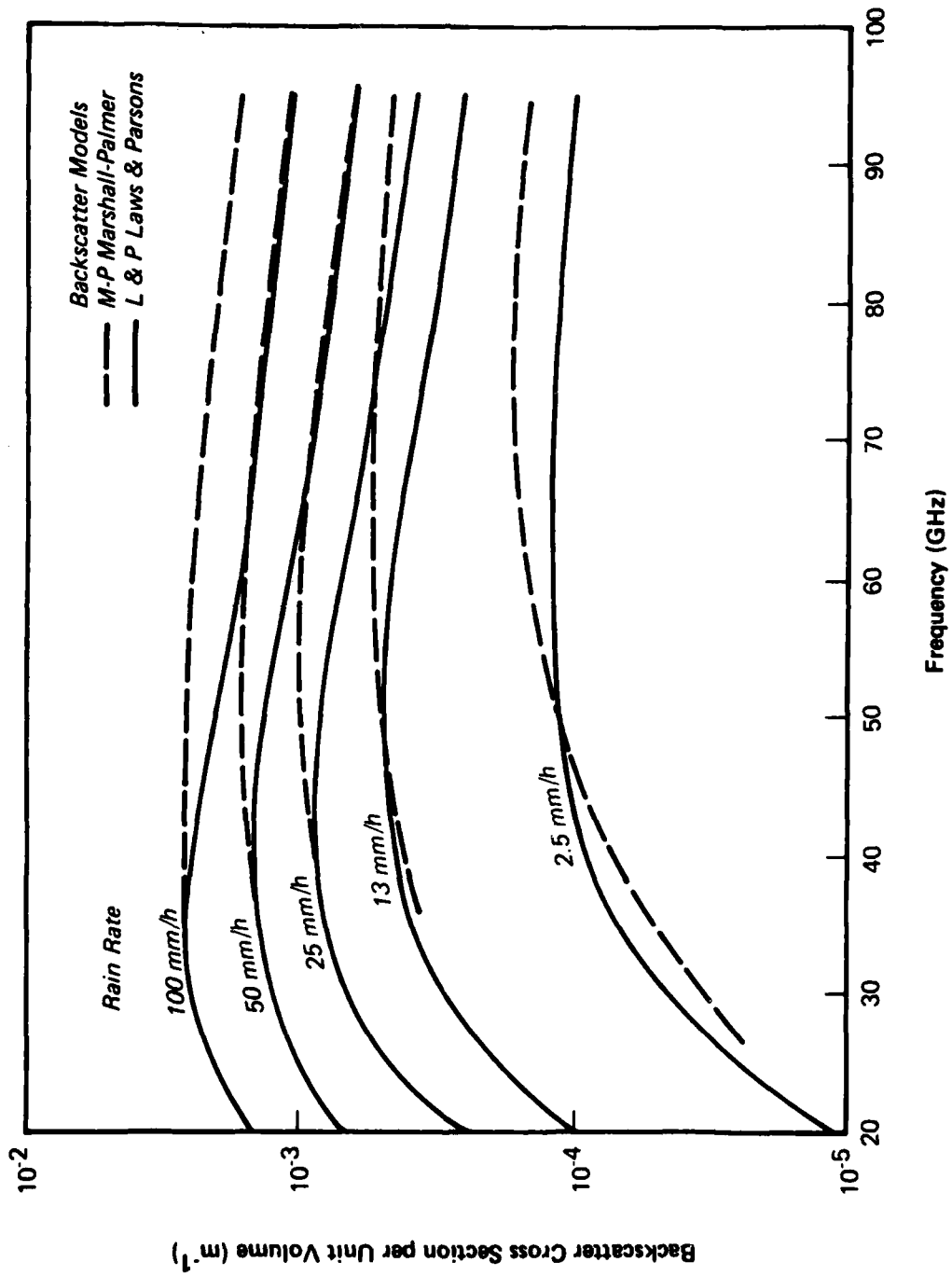


Figure 2 Reflectivity vs Frequency for Rain

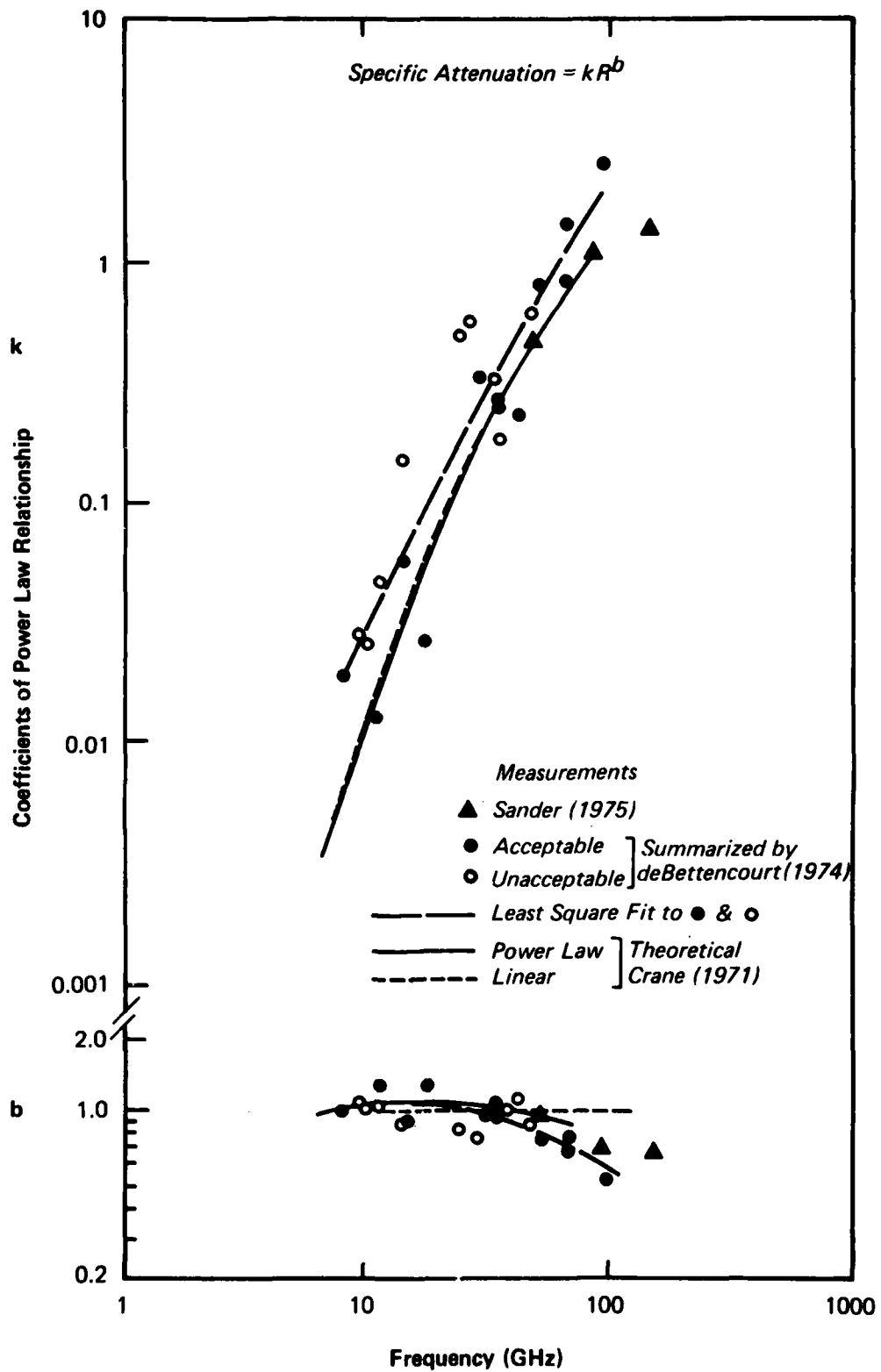


Figure 3 Coefficients of Power Law Relationships Between Specific Attenuation and Rain Rate

upon individual drop size distribution measurements reported by Crane (1971). The theoretical data are close to the L&P distribution results. The k and b coefficients in the power law relationship between specific attenuation and rain rate show good agreement between observations and theory at frequencies up through 100 GHz.

Multiwavelength radar measurements by the Ballistic Research Laboratories (BRL) at McCoy AFB in Florida show a similar good agreement between measured and estimated specific attenuation values at both 70 and 95 GHz. The raw observations obtained from Richard and Kammerer (1975) together with the theoretical calculations made using both the L&P and M-P distributions are presented in Figures 4 and 5 for 70 and 95 GHz, respectively. With the exception of some apparently spuriously low values of specific attenuation at rain rates between 1 and 10 mm/h, the agreement is good. The data were obtained by comparing the cross section of a corner reflector observed during rainy conditions with the cross section expected in the absence of rain. Considering that the rain was not measured along the relatively short path (450 m) but only at the target and that the measurements depend upon the radar calibration, the agreement is excellent.

2.2 Backscatter

Very little data exist for the verification of the theory for the estimation of the backscatter cross section per unit volume for frequencies above 20 GHz. However, adequate checks on the theory have been made at lower frequencies and no complications exist which could invalidate the theory at one frequency after it has been validated at another. The multiwavelength data obtained by BRL do provide additional evidence and support for the theoretical calculations at higher frequencies. Figures 6 through 13 provide summaries of the cross section measurements made by BRL at 9.4, 35, 70, and 95 GHz. The measurements displayed in Figures 6 through 9 are reproduced from the report by Richard and Kammerer (1975). The measurements displayed in Figures 10 through 13 are reproduced from the companion report by Currie et al (1975). The two sets of figures represent two different analyses of the same data.

Richard and Kammerer reduced A-scope photograph data. They determined the peak rain reflectivity from the A-scope data using the radar

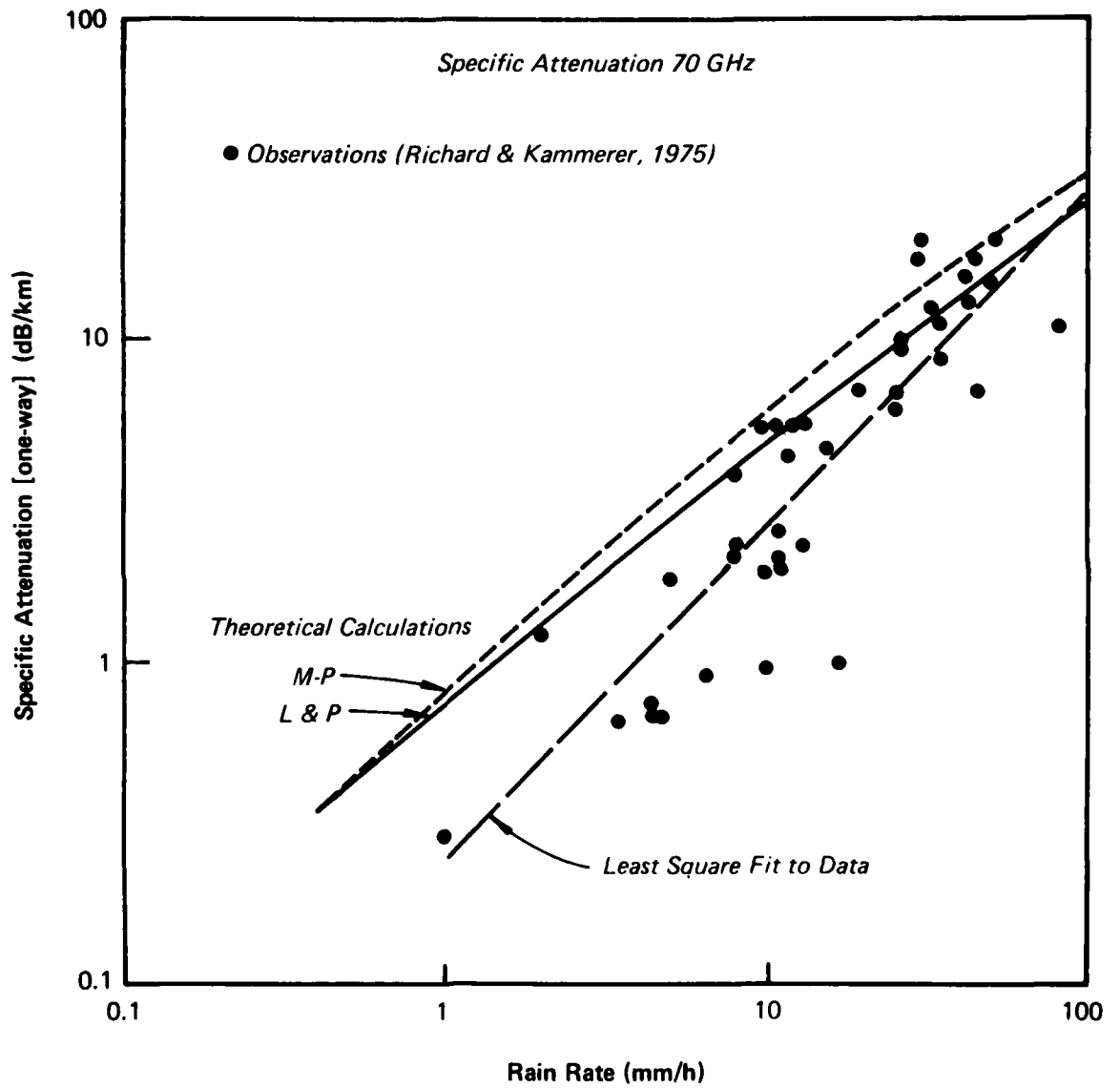


Figure 4 Specific Attenuation Observations at 70 GHz

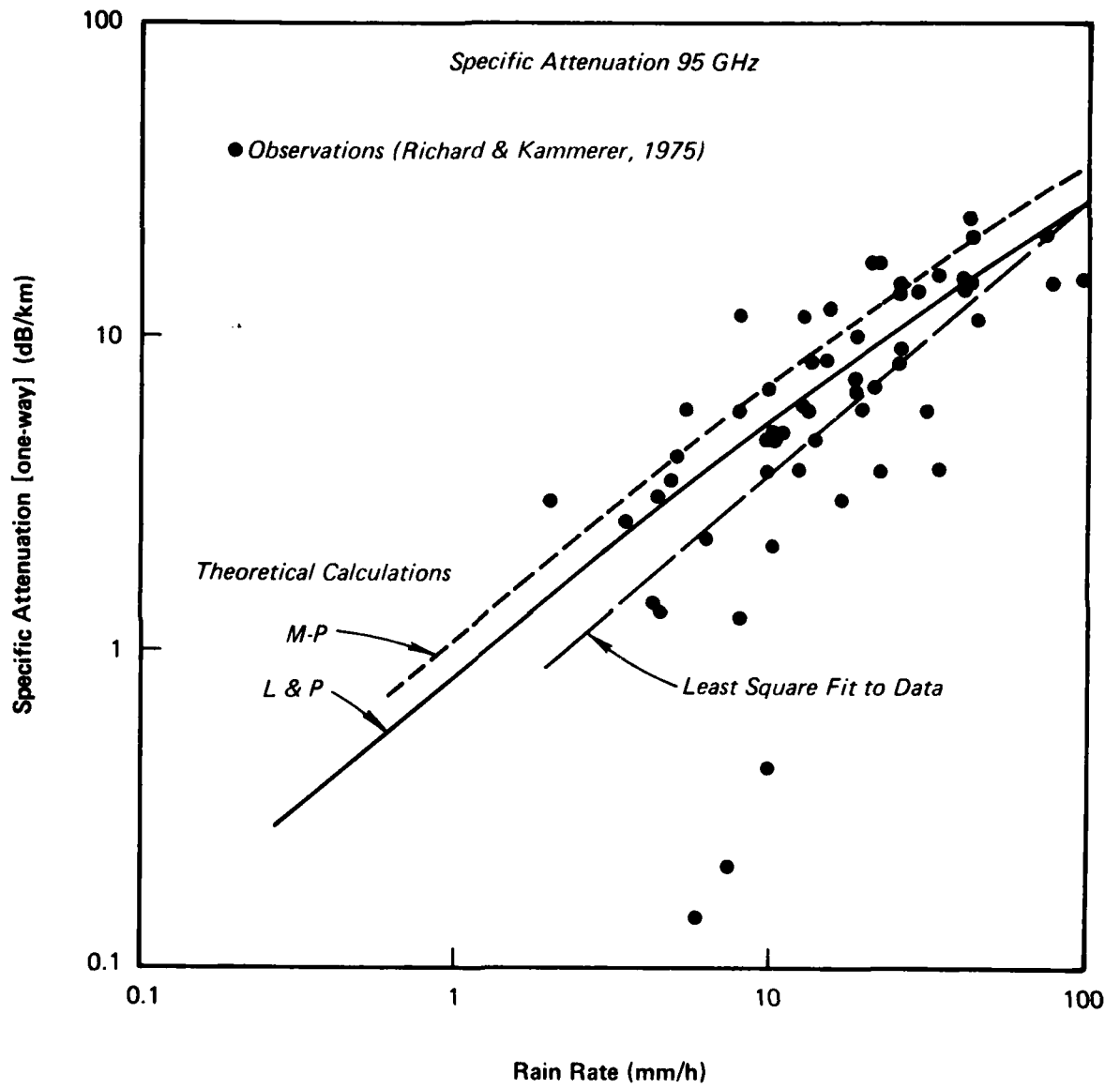


Figure 5 Specific Attenuation Observations at 95 GHz

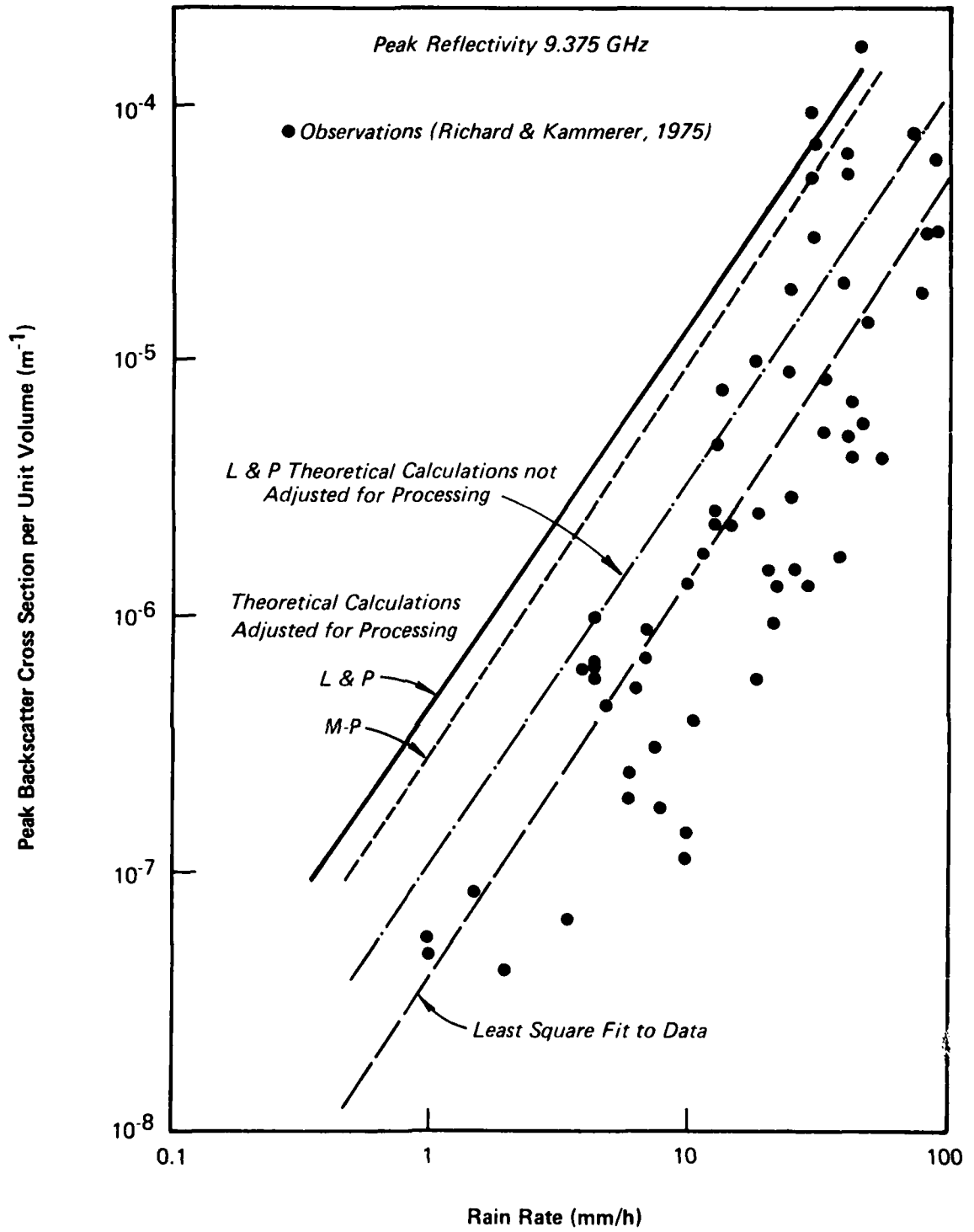


Figure 6 Peak Reflectivity Observations at 9.375 GHz

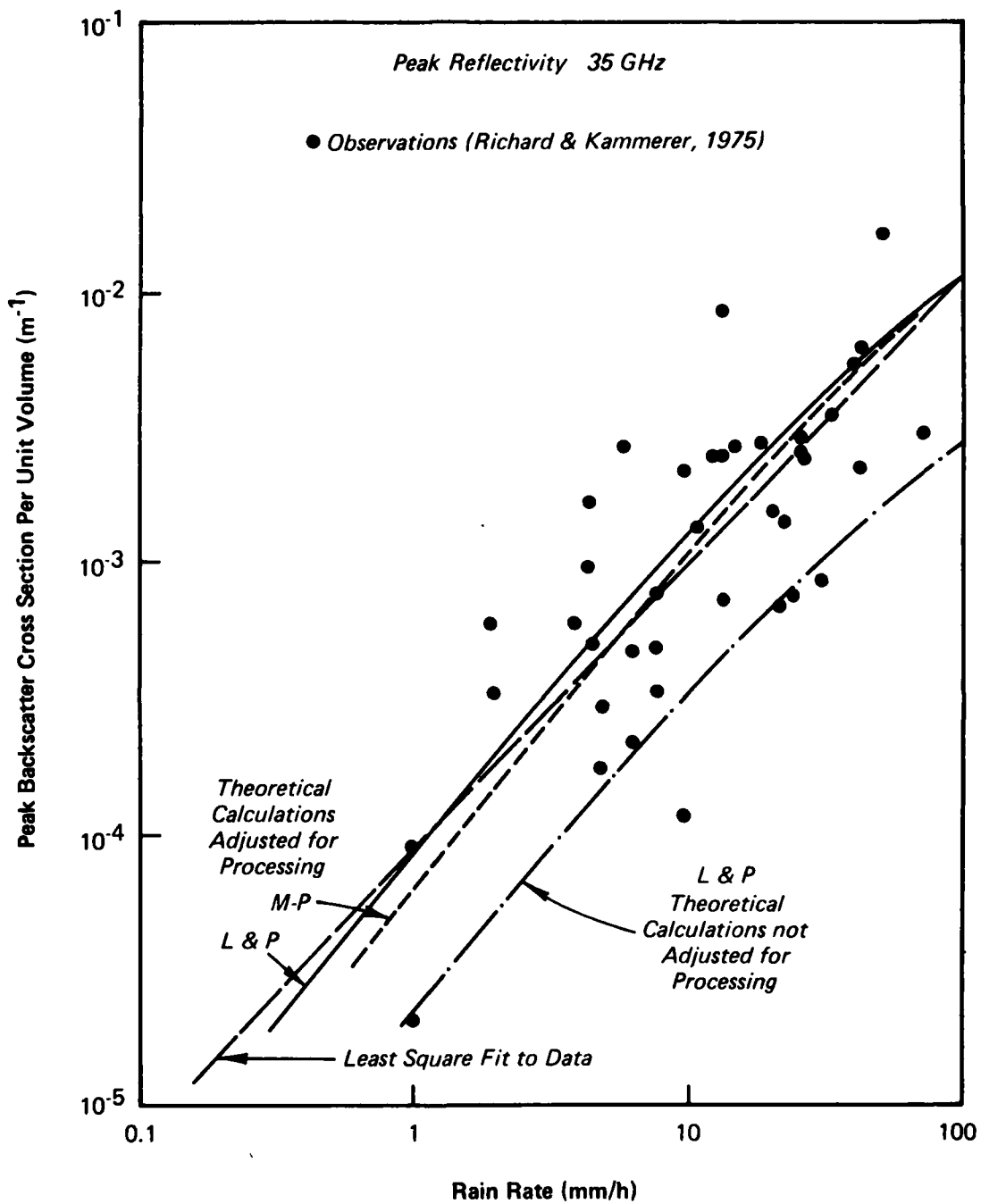


Figure 7 Peak Reflectivity Observations at 35 GHz

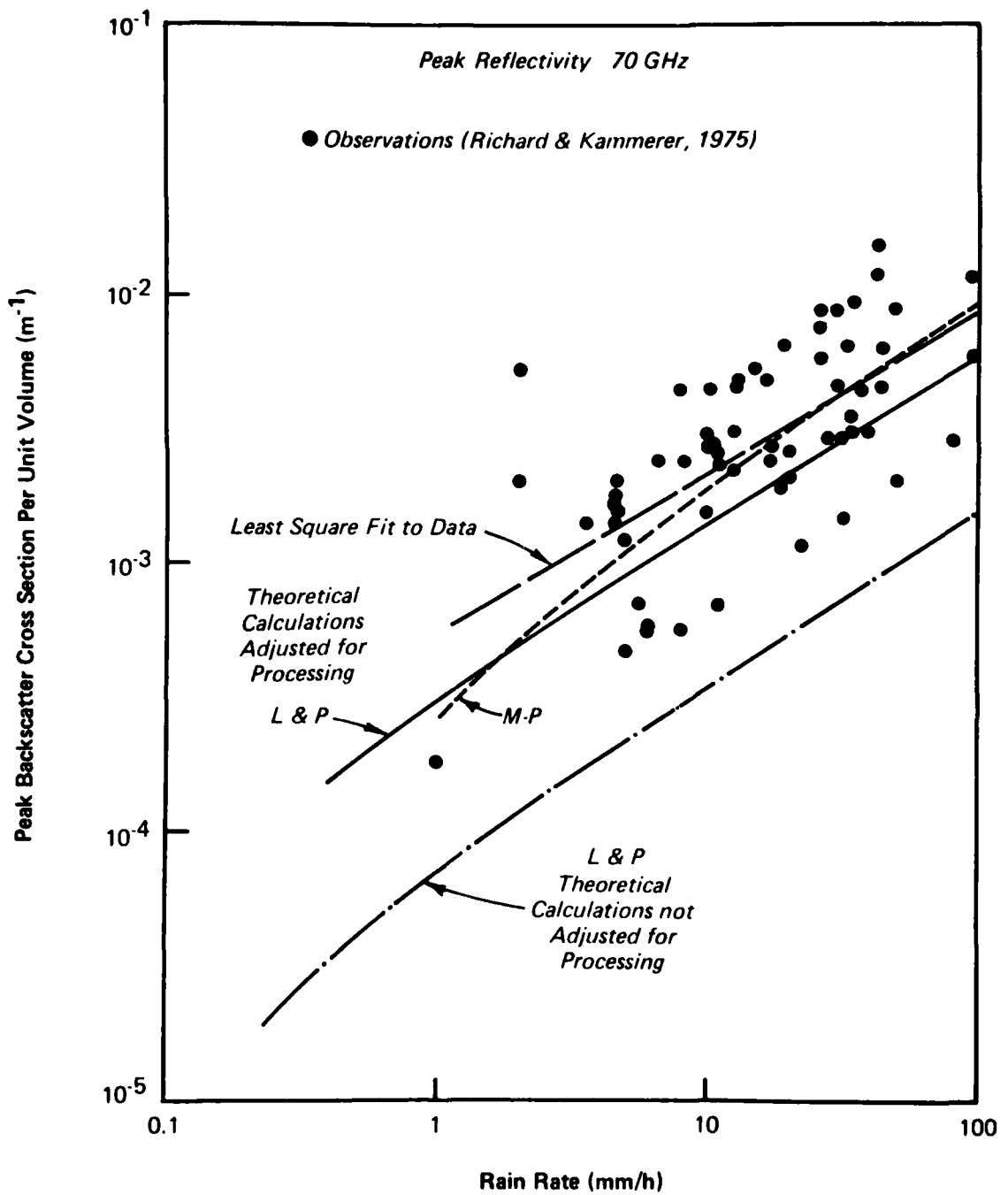


Figure 8 Peak Reflectivity Observations at 70 GHz

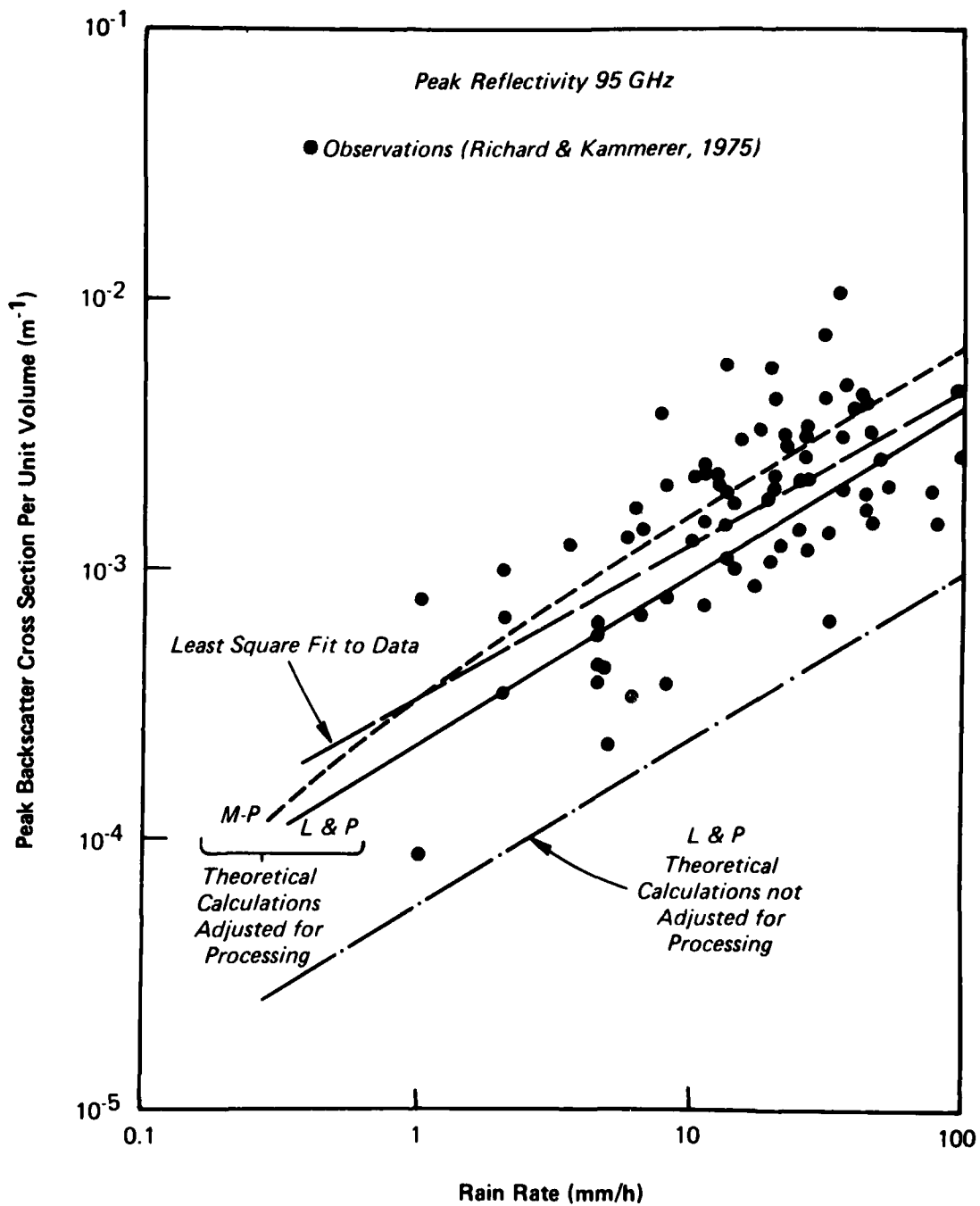


Figure 9 Peak Reflectivity Observations at 95 GHz

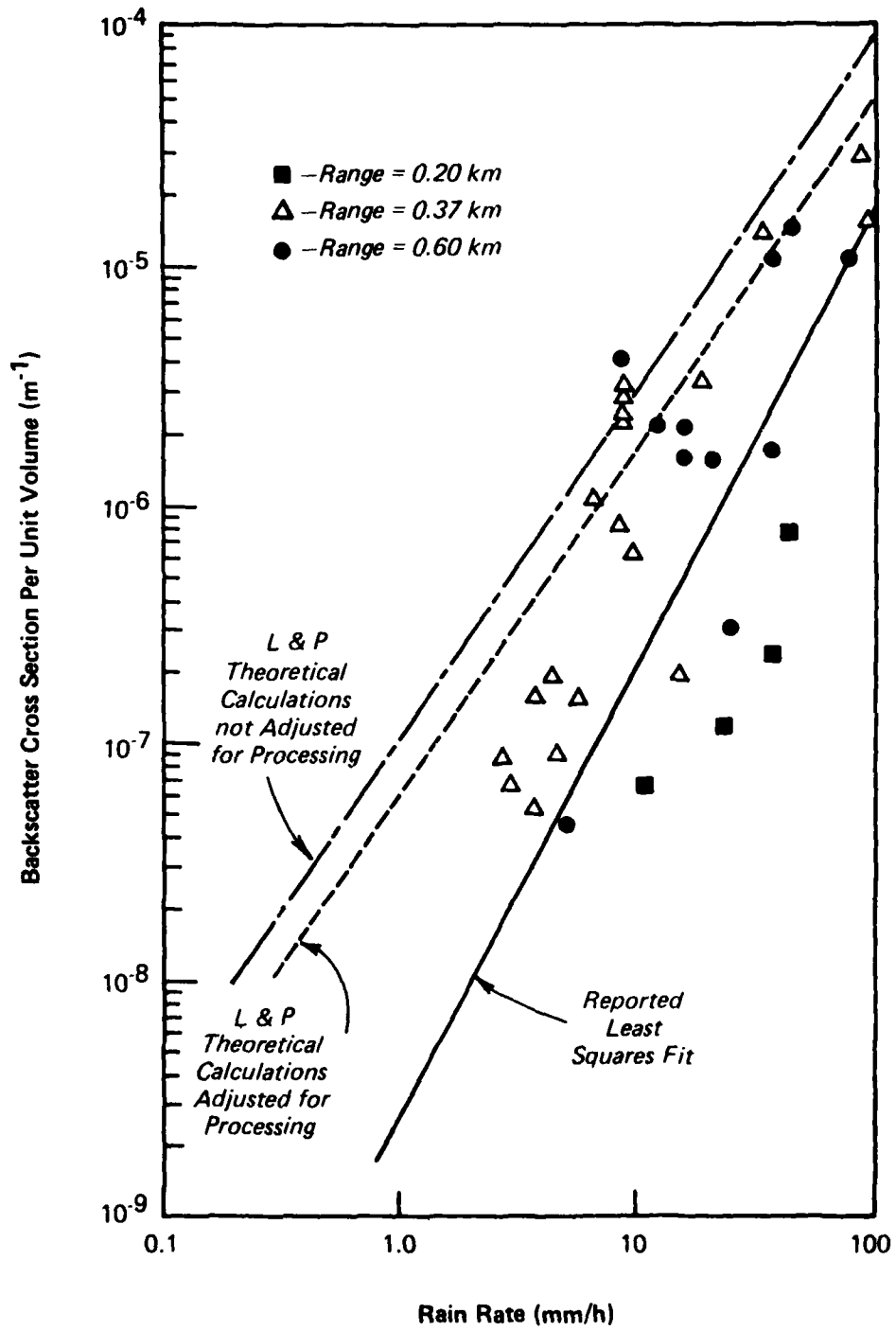


Figure 10 Average of the Logarithm of Reflectivity
 Obtained by Carrie et al (1975) at
 9.375 GHz

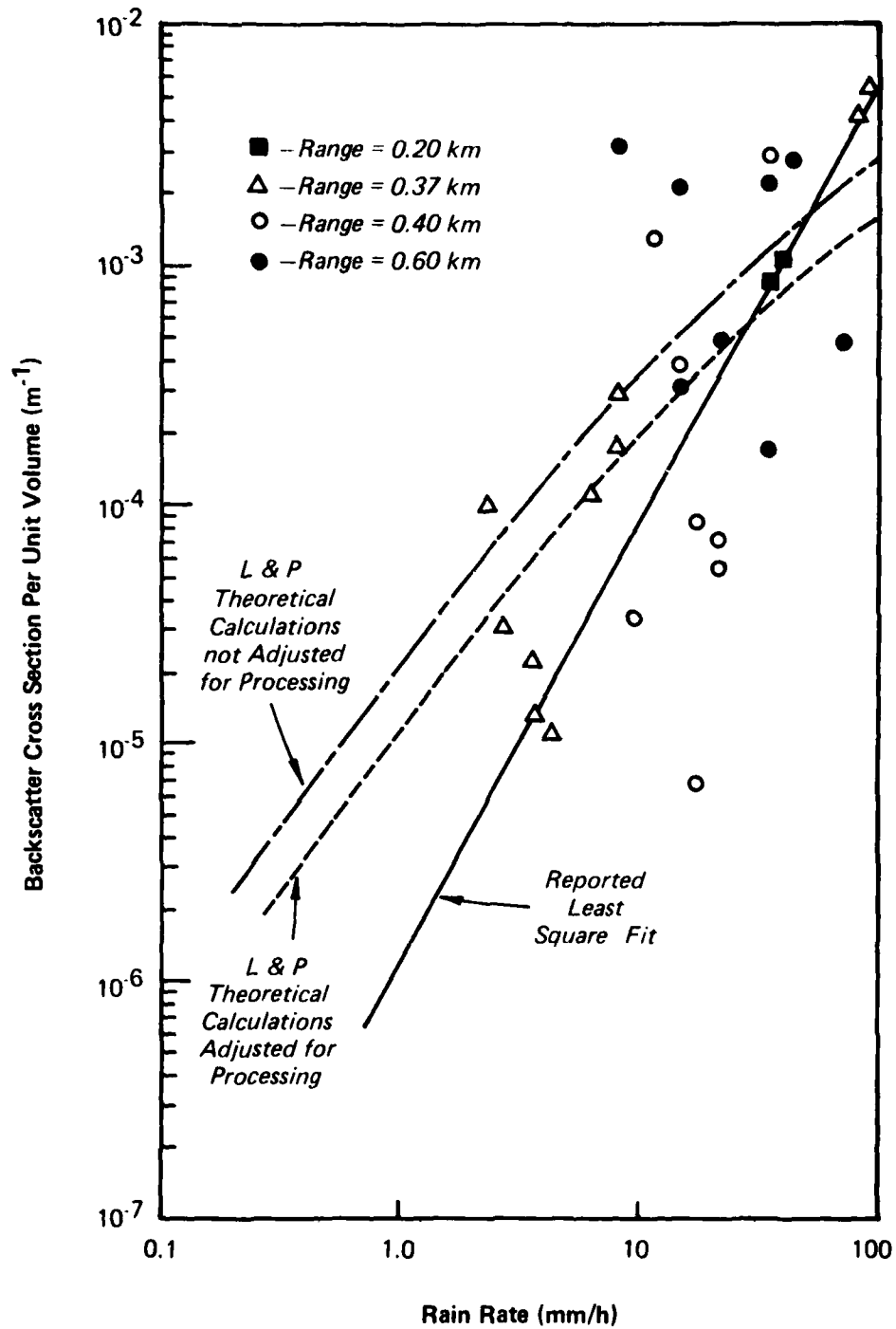


Figure 11 Average of the Logarithm of Reflectivity Obtained by Currie et al (1975) at 35 GHz

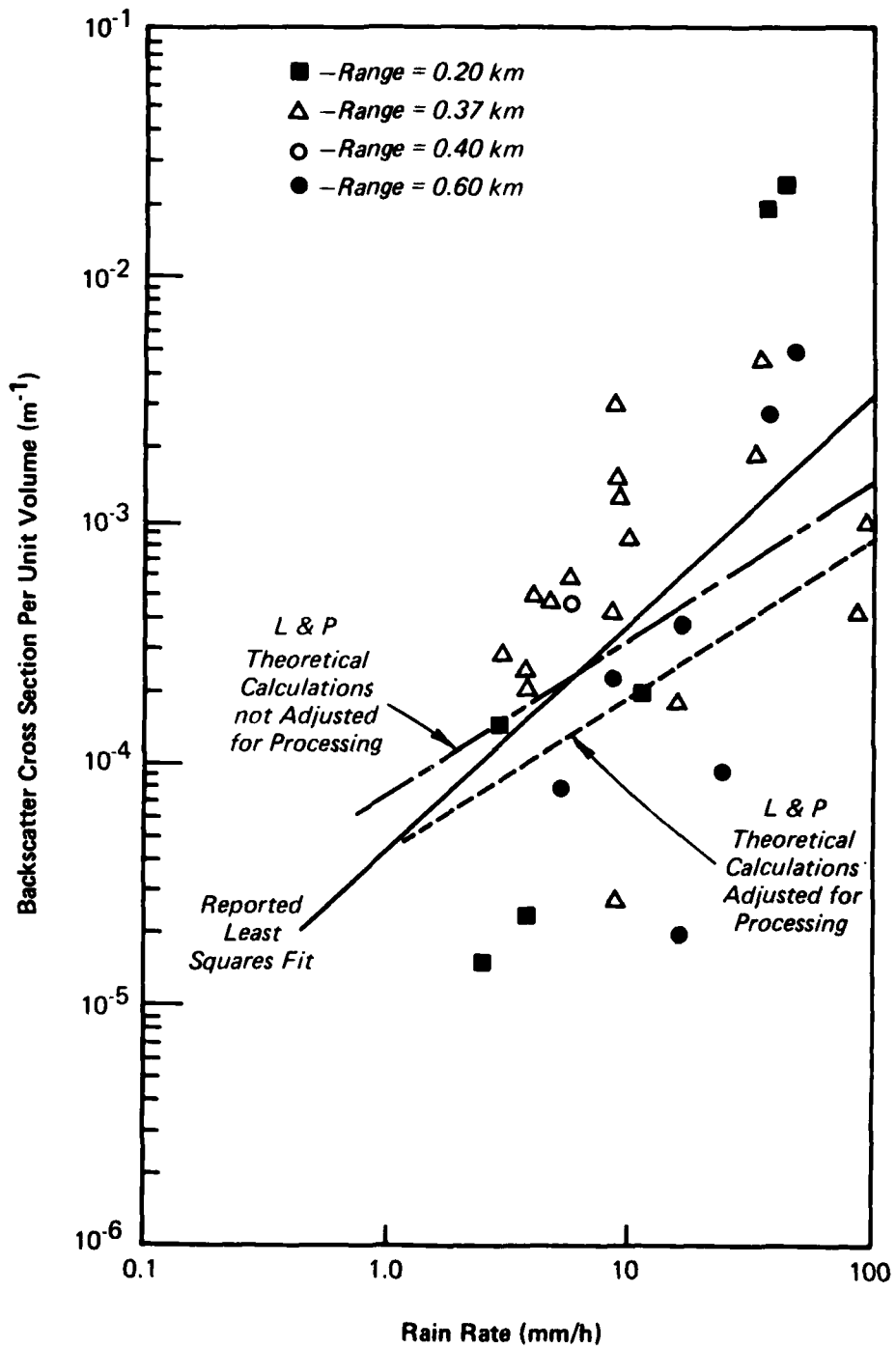


Figure 12 Average of the Logarithm of Reflectivity Obtained by Currie et al (1975) at 70 GHz

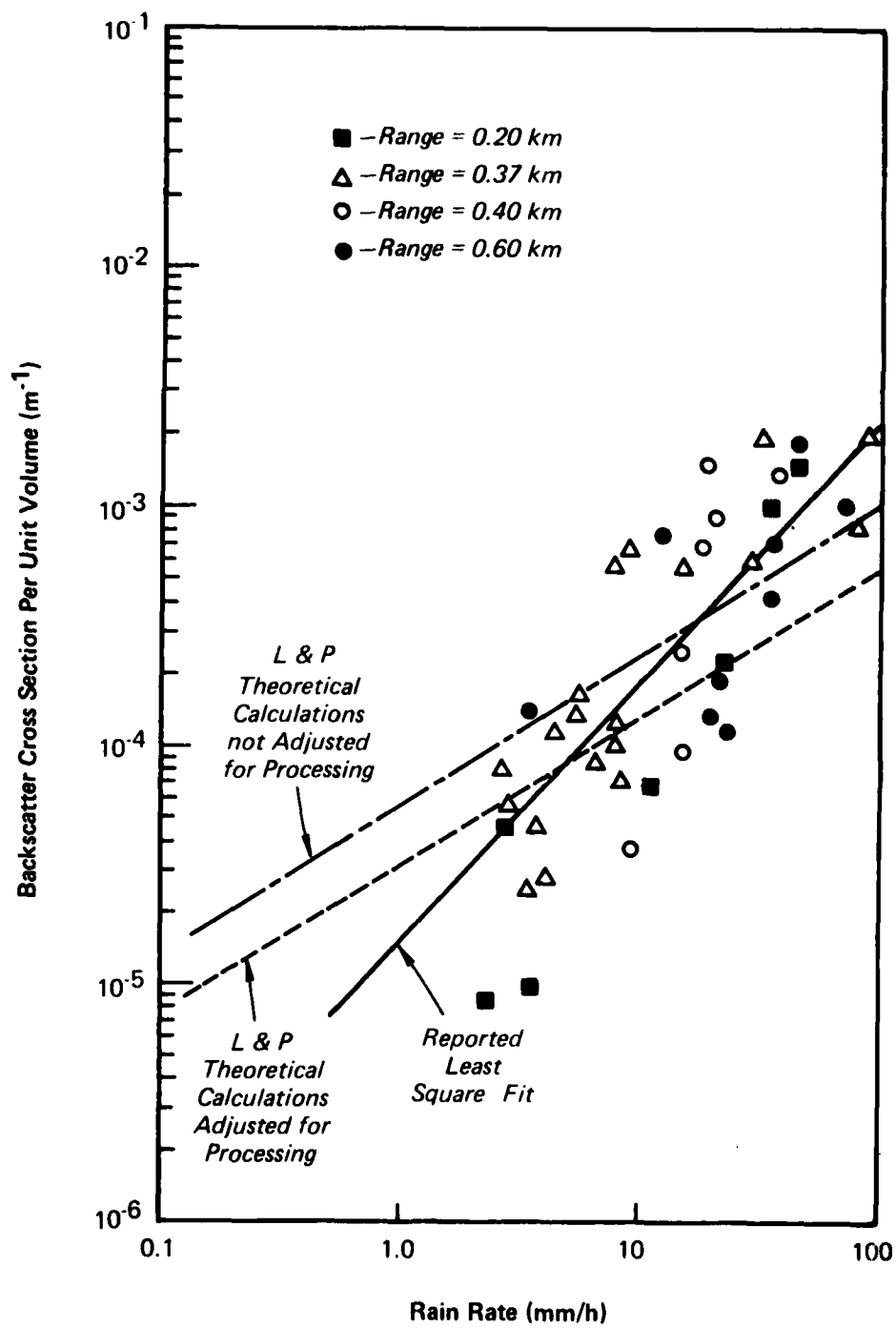


Figure 13 Average of the Logarithm of Reflectivity Obtained by Currie et al (1975) at 95 GHz

returns from range intervals in front of and behind the corner reflector and reported the peak backscatter cross section per unit volume for the range to the corner reflector. Precise radar calibration and attenuation estimation were not necessary since the corner reflector cross section value was corrected for possible rain contamination and the peak rain cross section value was calculated using the known cross section of the corner reflector as reference. The processing adjustment made to the theoretical calculations prior to comparison with the observations in the figures is required to compensate for the use of the peak value instead of the logarithm of the average reflectivity as assumed in most theoretical analyses. The unadjusted L&P curves are also presented for comparison. From prior experience, it is known that the signal return (pulse to pulse variation) from rain has a Rayleigh distribution (Atlas, 1964). The highest signal value from 50 independent samples from a Rayleigh process is 6 dB above the mean (for a linear receiver, e.g. see Crane, 1973). Since roughly 50 independent pulses were sampled in the process of detecting the peak value, a 6 dB adjustment was used for the theoretical calculations plotted in Figures 6 through 9. Richard and Kammerer experimentally determined the adjustment to be 5.9 dB.

The data reported by Currie et al (1975) were obtained from the same set of measurements on the same radars as the BRL results. They used magnetic tape recorded A/D output from the logarithmic receiver at a single range gate which could be moved in range. In post processing analysis, they averaged the recorded output and converted the values directly to cross section per unit volume estimates. In transforming to reflectivity estimates the path attenuation had to be estimated and used to correct the radar observations. They used the empirical relationship of deBettencourt (1974) and the measured surface rain rate values to make the attenuation estimates. Since that relationship tends to overestimate attenuation (see Figure 3), the correction will produce reflectivity estimates that are too high at high rain rates. This tendency is evident in their data. The data also were not adjusted for the difference between the average of power and the average of the logarithm of the power for a Rayleigh process (Atlas, 1964). This last adjustment (2.5 dB) has been included as a correction to the theoretical calculations on the figures presented in this report. Since the data reported by Currie et al require

both a precise radar calibration and precise attenuation correction (the total attenuation values are as large as 10 dB two way for the 450 m path at rain rates in excess of 10 mm/h) they are considered to be less reliable than the BRL results and will not be considered further in this report.

The BRL measurements (Figures 6-9) are in excellent agreement with the adjusted theoretical calculations at frequencies of 35 GHz and above. The theoretical calculations are known to be valid at 9.4 GHz although the BRL data show otherwise. The 9.4 GHz measurements are, however, highly suspect because the corner reflector had a relatively low cross section at this frequency and the antenna beamwidth was not large enough to suppress sidelobe contamination and multipath effects. BRL claims that the latter problems were significant at low rain rates. At 35 GHz, the reported least square fit power law relationship for the BRL observations is within 2 dB of the adjusted theoretical calculations. At 95 GHz, the reported least square fit power law lies between the two sets of adjusted theoretical calculations (L&P and M-P). It is known that the L&P distributions tend to underestimate the number of small drops while the M-P distribution tends to overestimate the number of small drops. Based on experience, the observations should lie between the two distributions. However, the precision of the BRL measurements is not great enough to select one drop size distribution model over the other.

In conclusion, a careful examination of the available observations is sufficient to reveal the veracity of the theoretical calculations. Insufficient data are available to select the best drop size distribution for use with the theoretical calculations. Since the drop size distribution may change from one location to another depending upon the existence of ice aloft in the storm, the relative humidity of the environment surrounding the falling drops, and the presence of low level clouds or fog, the establishment of the appropriate drops size distribution is a meteorological problem, not a question of the adequacy of the theoretical model.

3. THEORETICAL MODEL FOR PROPAGATION THROUGH CLOUDS

The attenuation caused by either rain or clouds is a result of two phenomena - absorption and scattering. In this section, results are presented for the theoretical estimation of attenuation and backscatter cross section based on the use of a continuous distribution of cloud particle sizes within a given volume.

The full Mie theory of scattering has been applied in the millimeter wavelength range because the larger droplets have internal dimensions comparable in size to the wavelength in water. The use of the scattering properties of a single droplet in the description of the effects of cloud and rain also requires a model of the drop size distribution and an assumption about the statistics of drop location within a volume. The Gamma distribution is used for cloud droplet spectra. The drop size distribution is expressed as

$$N(r) = A r^{C_1} \exp \{-B r^{C_2}\}$$

where A and B are defined scale parameters, C_1 and C_2 are slope parameters and r is the drop radius.

Figure 14 shows the specific attenuation due to both water and ice clouds with liquid water contents of 0.2 and 2.5 cc/m³. The computations for ice are identical with those for water with the exception of differences in indices of refraction. The liquid water content also has to be interpreted as the ratio of the volume of ice to that of air in cc/m³. The index of refraction for ice is assumed to be constant, 1.78 - i(0.0024) throughout the millimeter wavelength range. For water, it varies from 5.243 - i(2.984) at 20 GHz to 4.0039 - i(2.5186) at 35 GHz and 2.7098 - i(1.4488) at 95 GHz. In the figure it is evident that the computed attenuation due to water clouds is over two orders of magnitude greater than for ice clouds with the same liquid water content. Furthermore, the attenuation at 95 GHz is higher than that at 35 GHz by a factor of 2 to 3 (3-4 dB) for all cases considered.

Figure 15 shows the computed backscatter cross sections per unit volume due to the same types of clouds. The relative differences in backscatter cross sections between water and ice clouds are less than those for attenuation. However, the frequency variation is more pronounced, an increase of close to two orders of magnitude from 35 to 95 GHz.

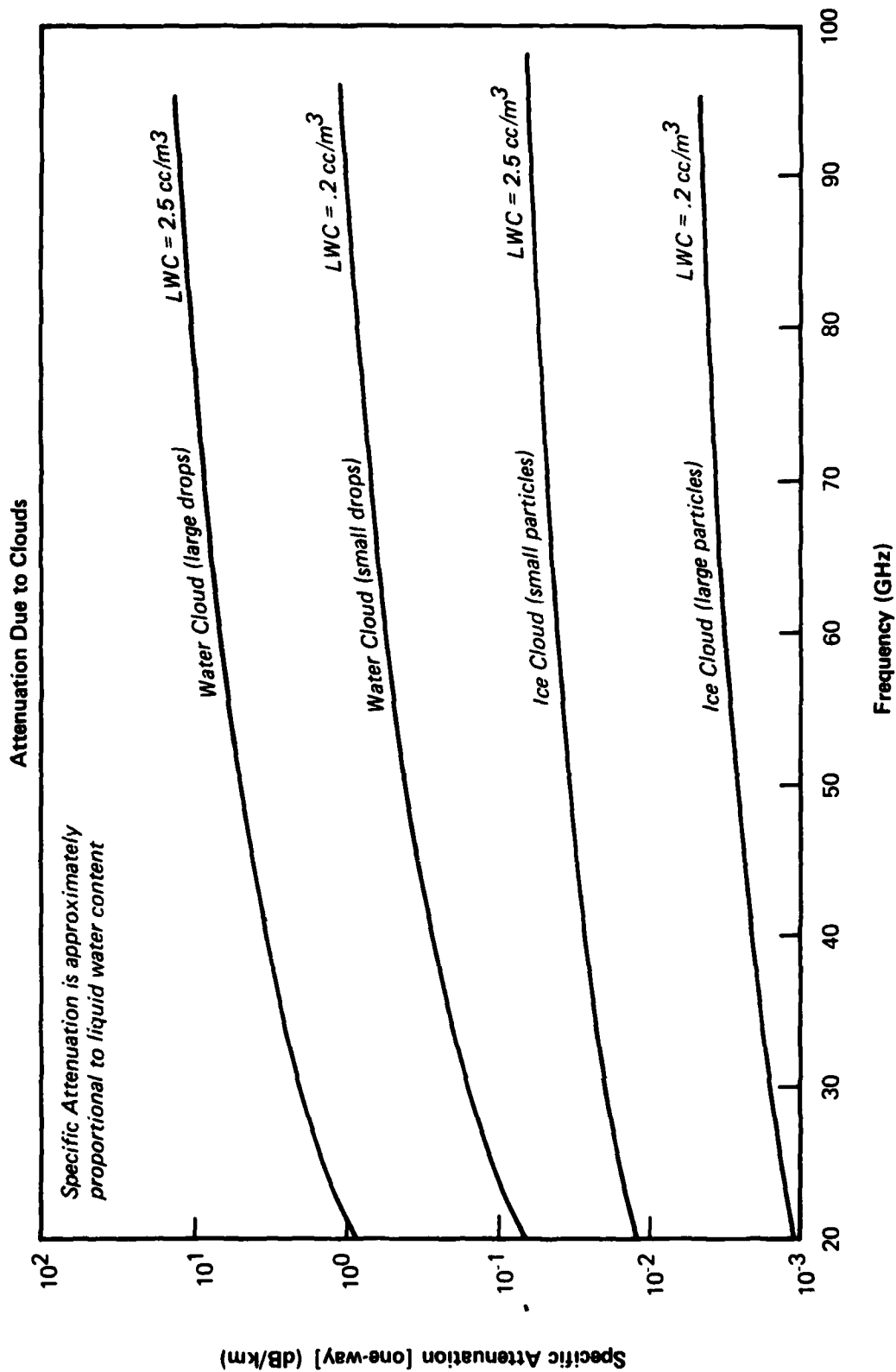


Figure 14 One Way Specific Attenuation vs Frequency for Cloud Particles

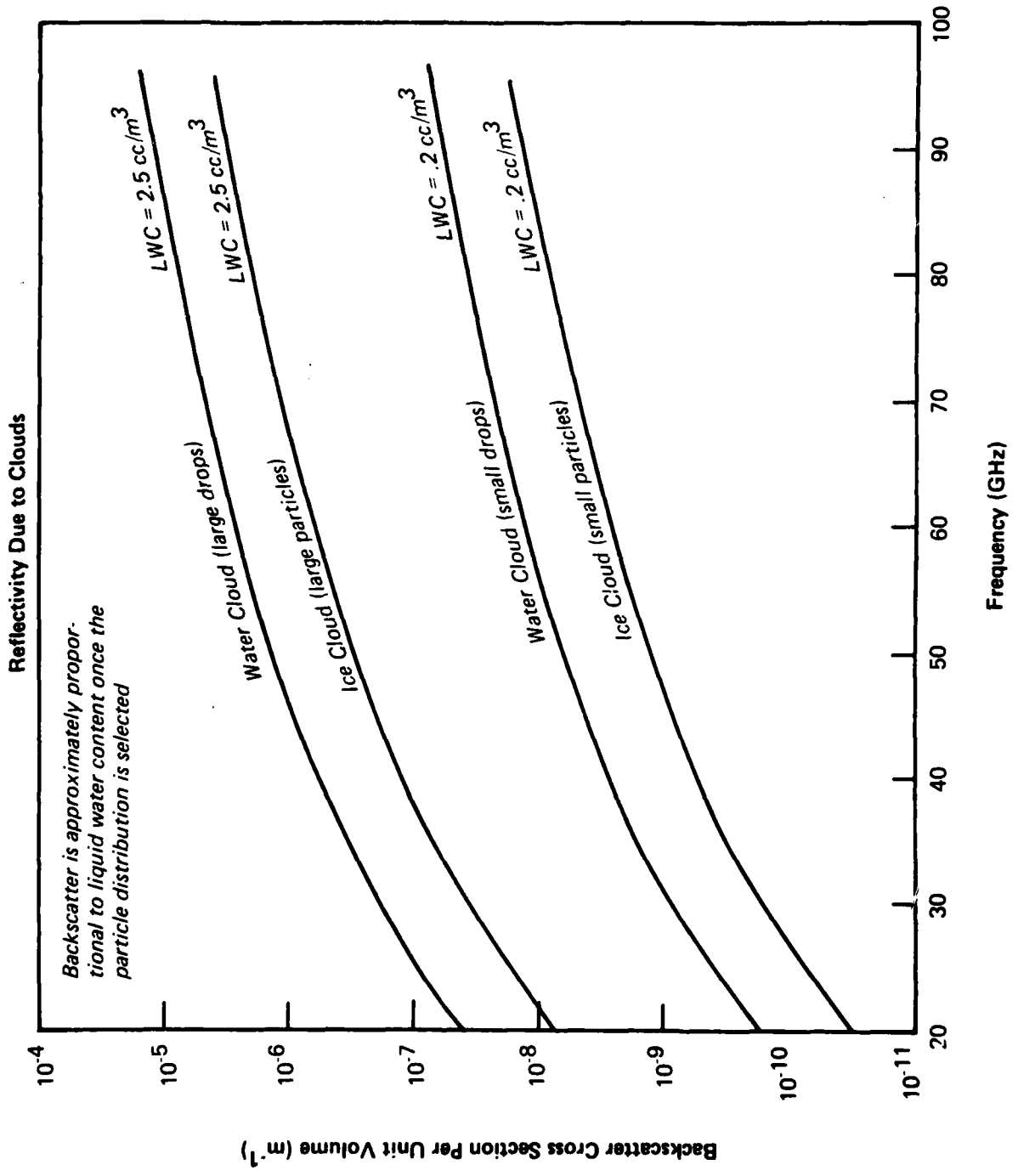


Figure 15 Reflectivity vs Frequency for Cloud Particles

Figure 16 is the uplooking brightness temperature for a standard mid-latitude atmosphere (spring/fall) with an integrated, columnar water vapor density of 1.9 gm/cm^2 and a low-lying stratus cloud (500 m - 1000 m) with liquid water content of 0.25 cc/m^3 . The result was obtained using the Gamma distribution relationship with $C_1 = 6.0$ and $C_2 = 1.0$. In comparison with Figure 17 for a clear atmosphere, there is little evidence of the effects of cloud at frequencies between 20 and 65 GHz. On the other hand, a substantial warming of more than 50°K is evident due to the presence of cloud at frequencies between 70 and 95 GHz. Figure 18 is the uplooking emission temperature for the same atmosphere as Figure 17 with a cirrostratus (ice) cloud inserted between 5000 and 7000 m. The cloud is composed of ice with an equivalent columnar liquid water content of 0.021 cc/cm^2 . There is no noticeable effect of the presence of the ice cloud because of the low attenuation by ice. Figures 19 and 20 are the uplooking brightness temperature values estimated for two different rain plus cloud conditions, rain at the surface of 4 mm/hr and 15 mm/hr, changing to cloud at the freezing level (2300 m). The cloud liquid water content was assumed to be 0.25 g/m^3 and the cloud was assumed to extend to the -10°C isotherm (3900 m). The warming effects indicating higher attenuation are especially pronounced at frequencies above 30 GHz.

Large ice particles which occur in sleet, or frozen rain, graupel, and hail produce pronounced variation in attenuation (Figure 21) and backscatter (Figure 22). For example, specific attenuation values are always lower for ice than for water at 35 GHz (see Figures 1 and 2 for water), but at 95 GHz the specific attenuation for ice are close to, or even higher than, those for water. It is also noted that the backscatter cross section values for water (rain) decrease from 45 GHz to 95 GHz while for ice, the trend is reversed.

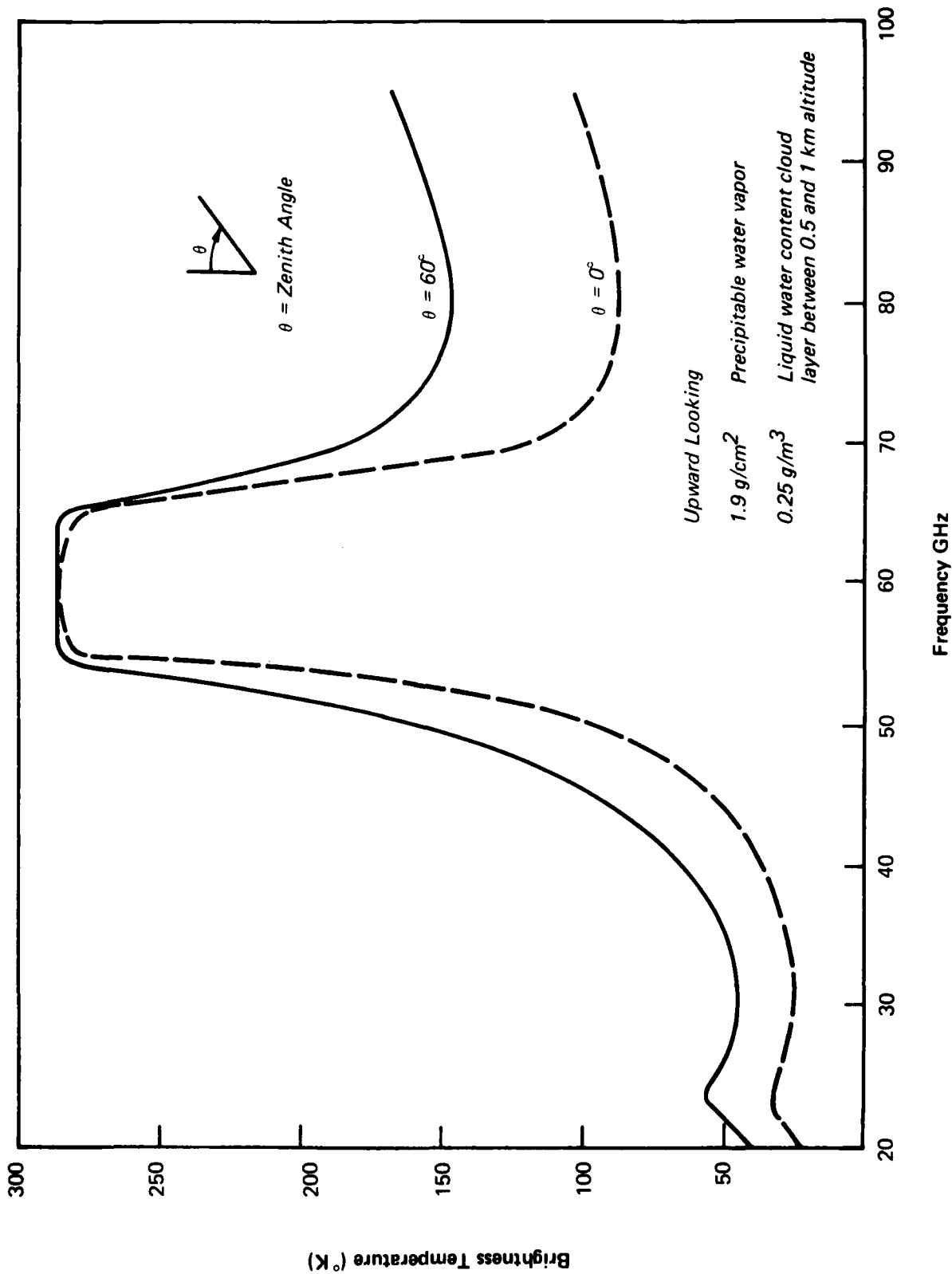


Figure 16 Brightness Temperature vs Frequency for a Cloudy Atmosphere (liquid water cloud particles)

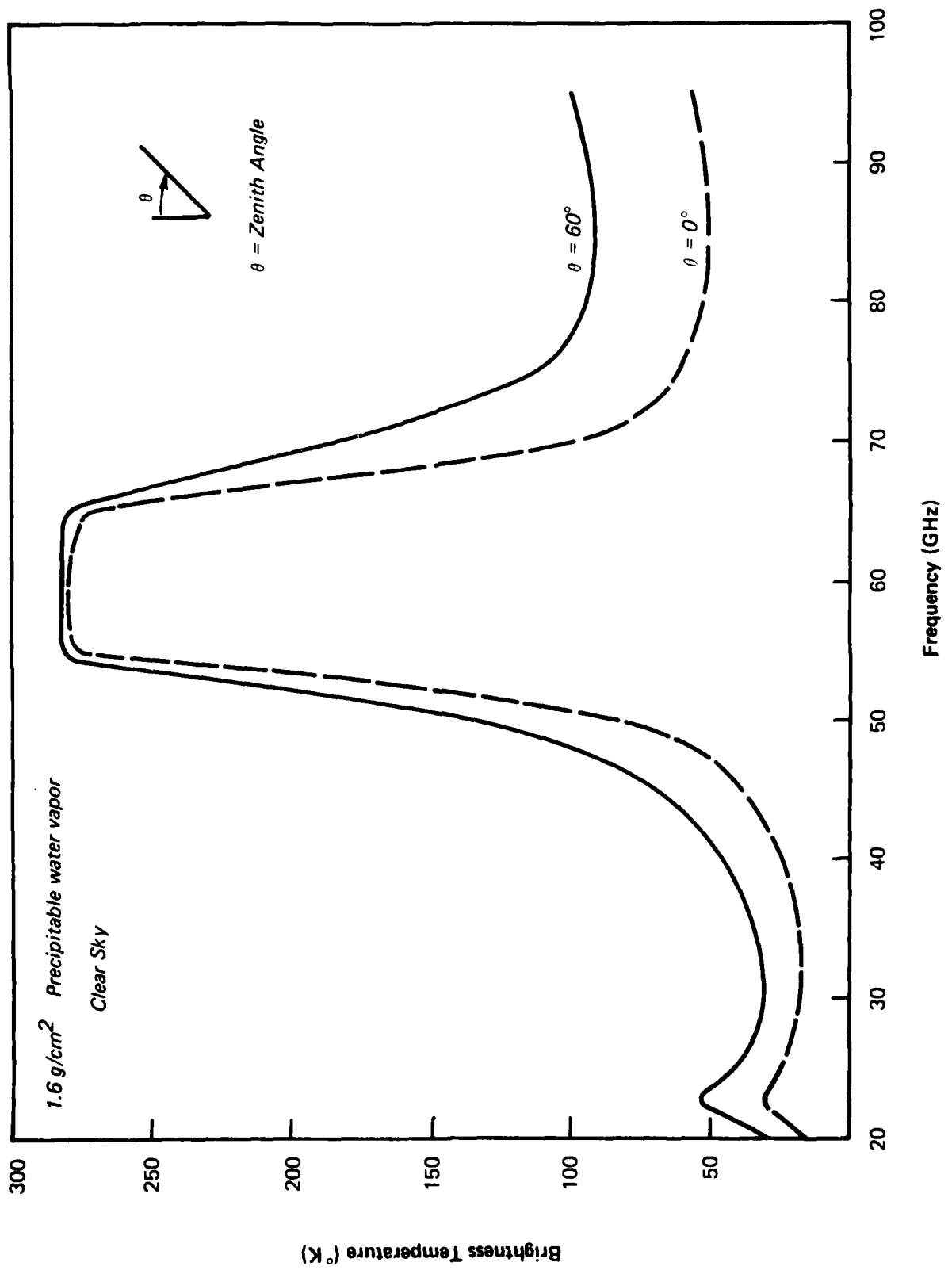


Figure 17 Brightness Temperature vs Frequency for a Clear Atmosphere

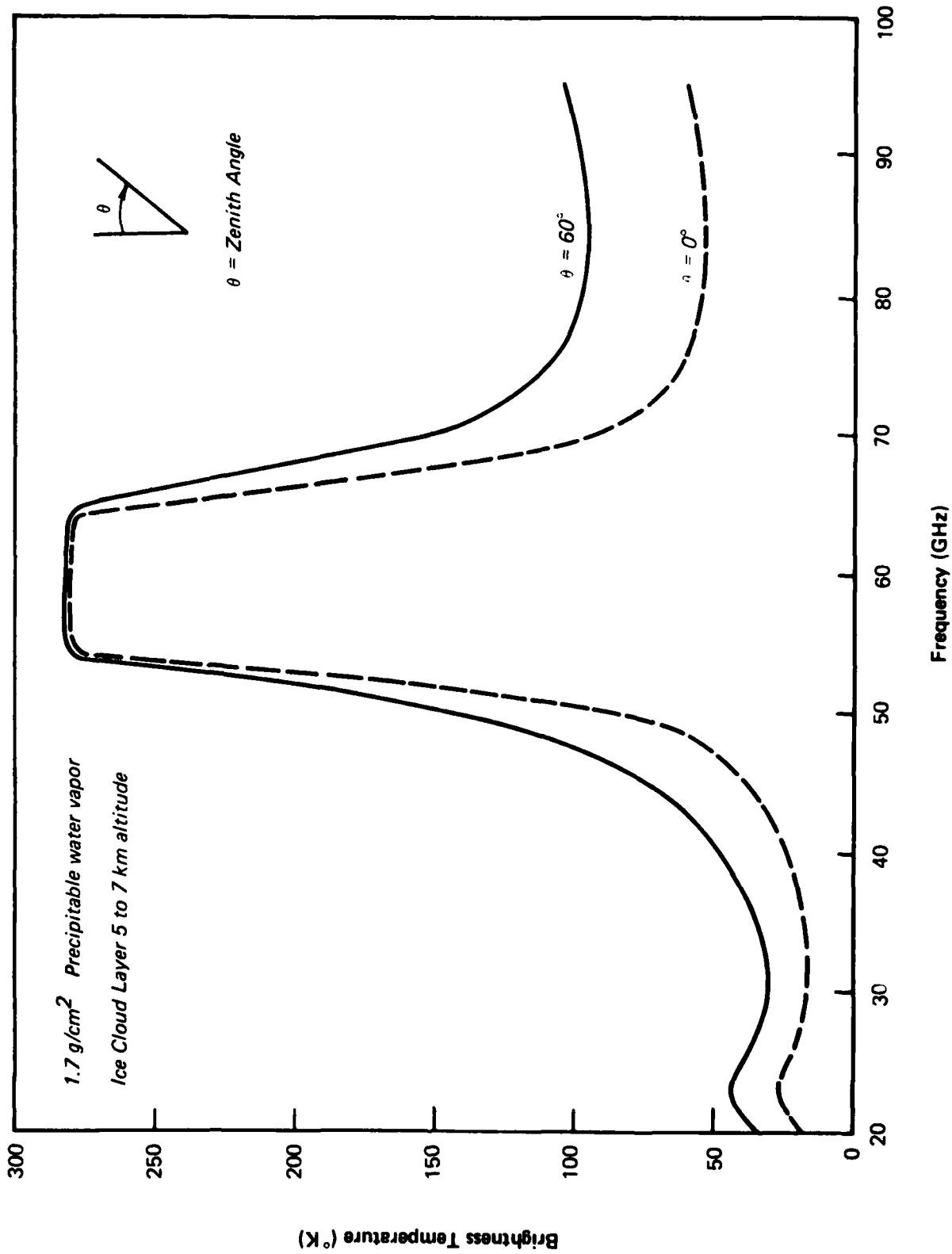


Figure 18 Brightness Temperature vs Frequency for a Cloudy Atmosphere (ice particles)

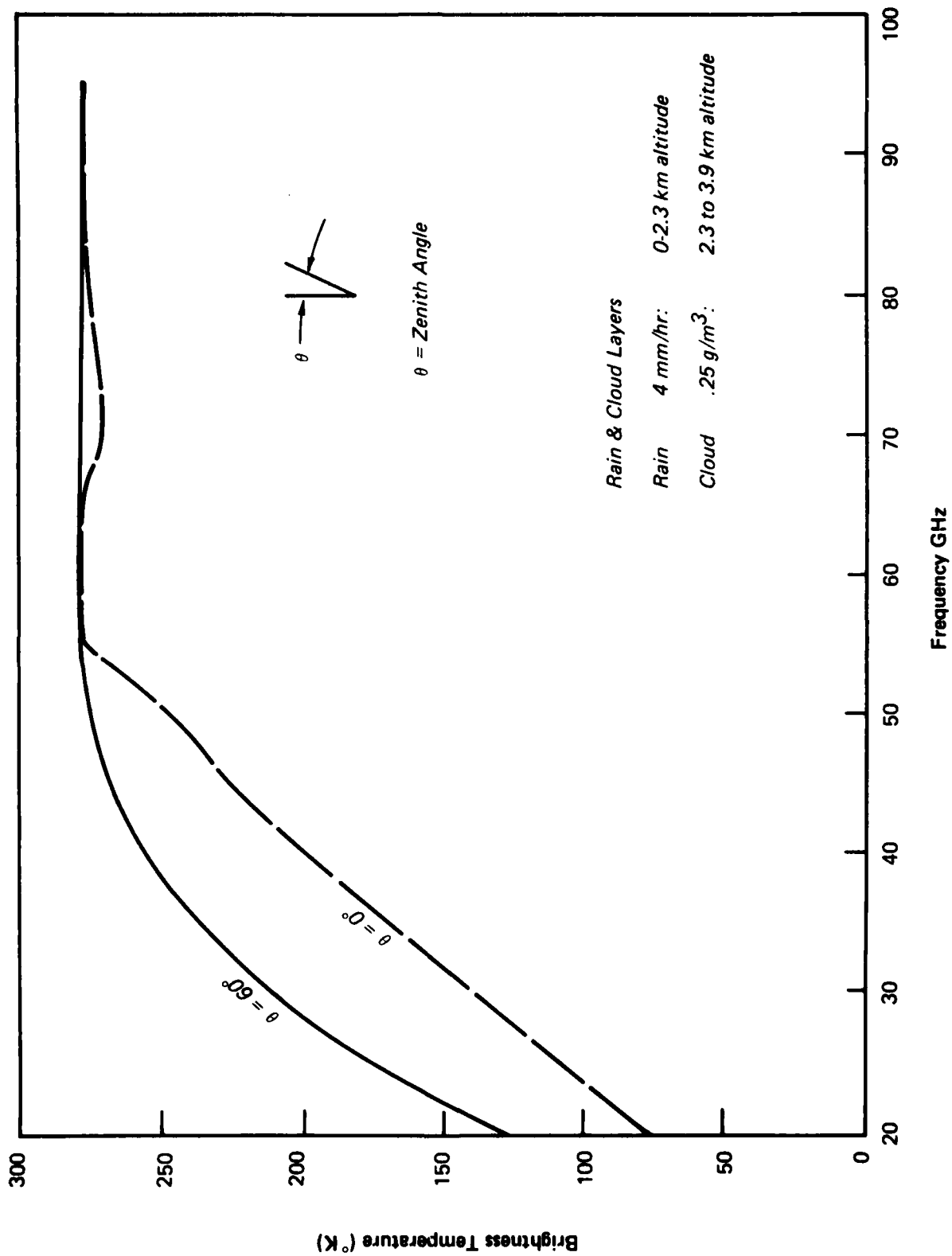


Figure 19 Brightness Temperature vs Frequency for a Light Rain Rate (4 mm/hr)

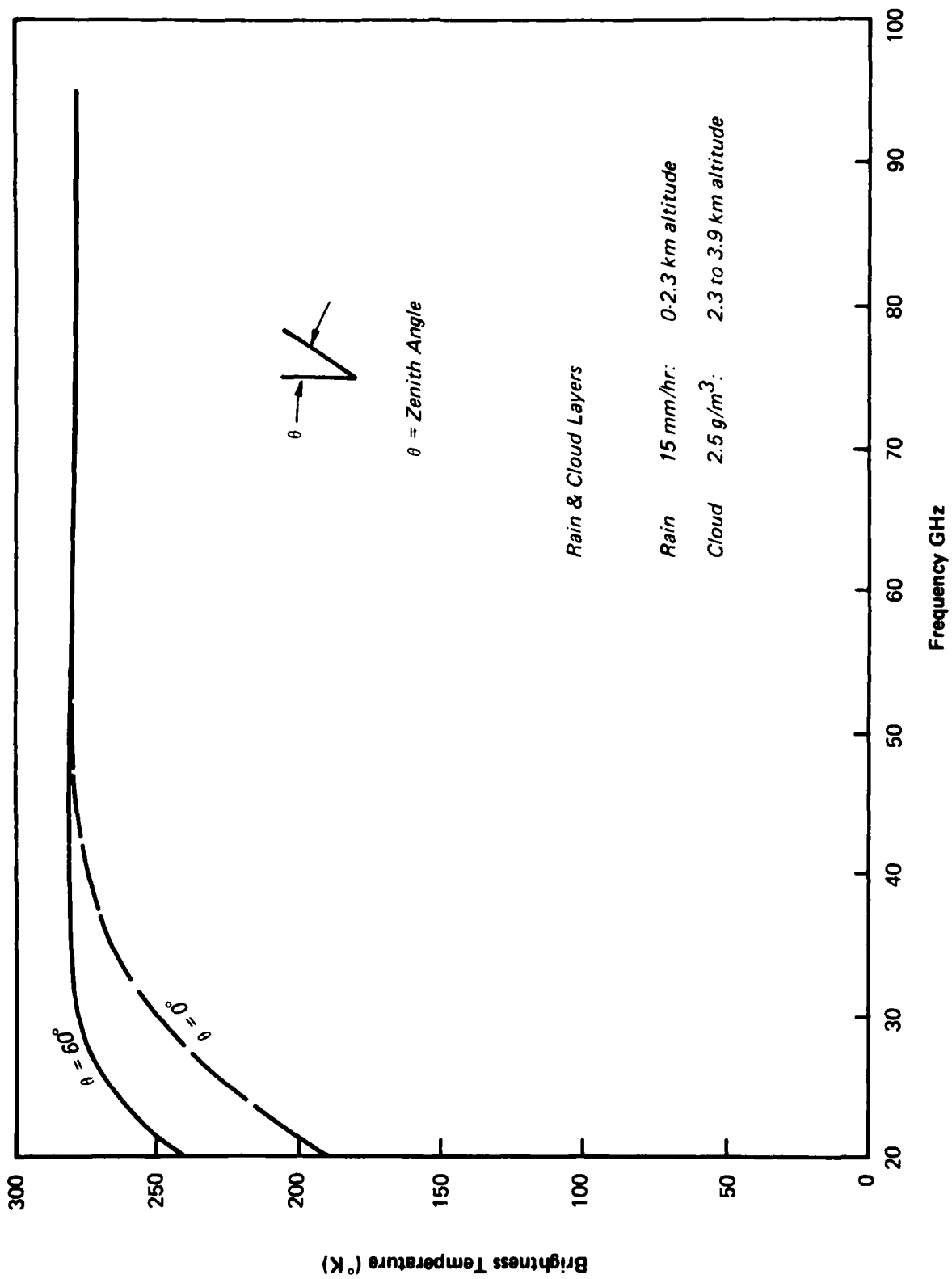


Figure 20 Brightness Temperature vs Frequency for a Moderate Rain Rate (15 mm/hr)

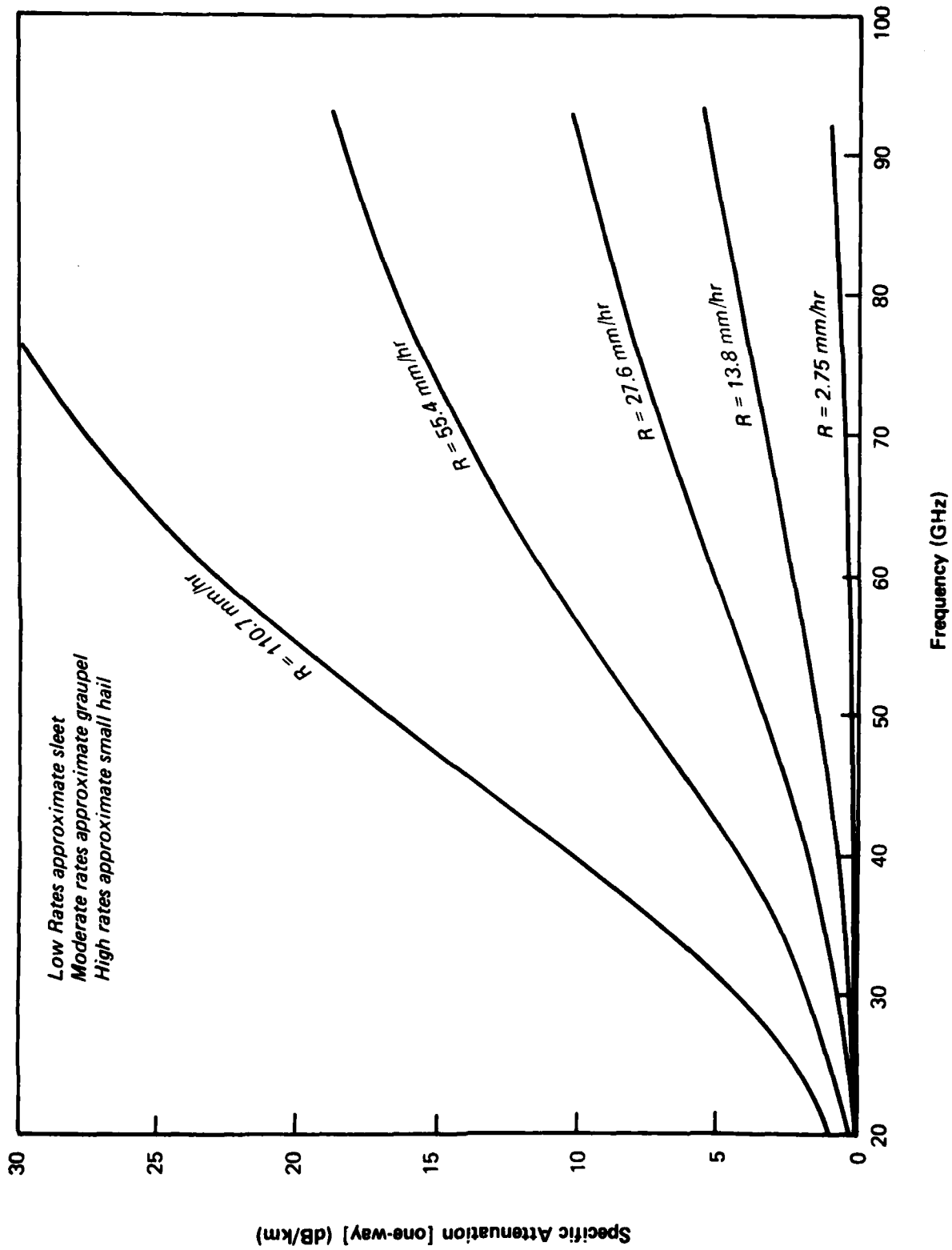


Figure 21 Specific Attenuation vs Frequency for Large Ice Particles

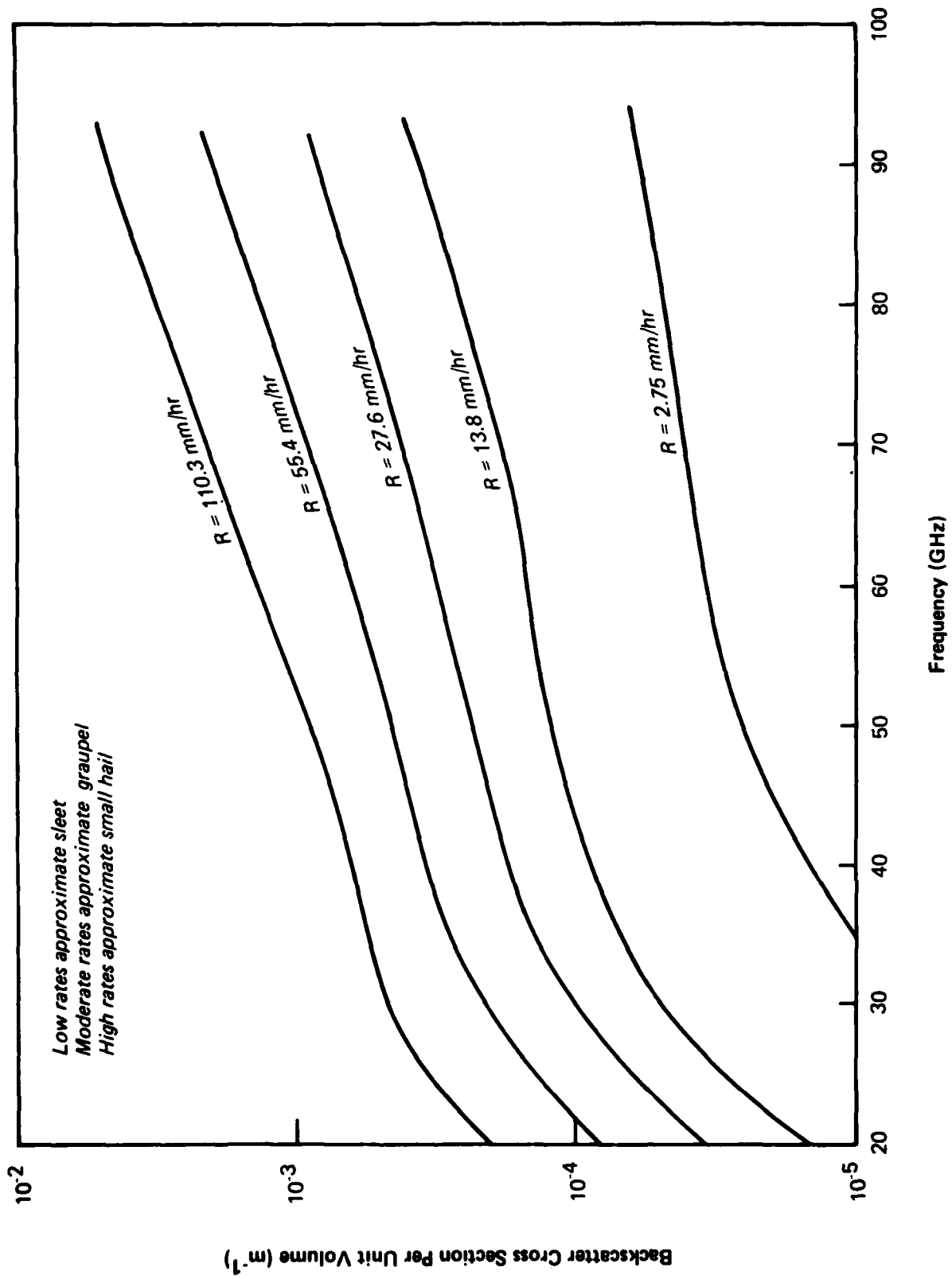


Figure 22 Reflectivity vs Frequency for Large Ice Particles

4. THEORETICAL MODEL FOR THE CLEAR ATMOSPHERE

The gases that absorb energy in the 20-95 GHz range in the atmosphere are oxygen and water vapor.

Water vapor, because of the electric polarity of the water molecule, produces rotation absorption lines at 22.2 GHz, 183 GHz and at higher frequencies. Its absorption is dependent upon the water vapor content of the atmosphere.

The total zenith attenuation in the vicinity of 60 GHz (Figure 23) is due primarily to the resonance of oxygen molecules caused by magnetic depole rotational transitions. The resonances occur at a number of frequencies within the 50 to 70 GHz range. Each resonance line is broadened by molecular collisions in a manner which is pressure and temperature dependent. As a result, in the 50 to 70 GHz range, these lines combine to form a continuous absorption region at a pressure of one atmosphere.

The most commonly used expression for theoretical line shapes was defined by Van Vleck and Weisskopf (1945). Recently, Rossencrantz (1975) improved the analysis for better agreement with measurements.

Figure 23 shows the water vapor, oxygen and total atmospheric attenuations for the clear midlatitude standard atmosphere (spring/fall) with an integrated water vapor content of 1.6 gm/cm^2 . It is evident that between 20 and 30 GHz the attenuation due to water vapor dominates. Between 45 and 70 GHz, the attenuation is due to oxygen with a sharp increase from 50 to 60 GHz and a sharp decrease from 60 to 70 GHz. In the 75 to 95 GHz range, there is little change in attenuation and the contribution from water vapor starts to dominate again.

Figure 17 shows the uplooking brightness temperatures as a function of frequency with the same atmospheric conditions as in Figure 23. Two zenith angles, 0° and 60° , are used to demonstrate the variation in atmospheric path lengths. It is shown that between 55 and 65 GHz the emission temperature stays almost constant indicating the effect of saturation by oxygen.

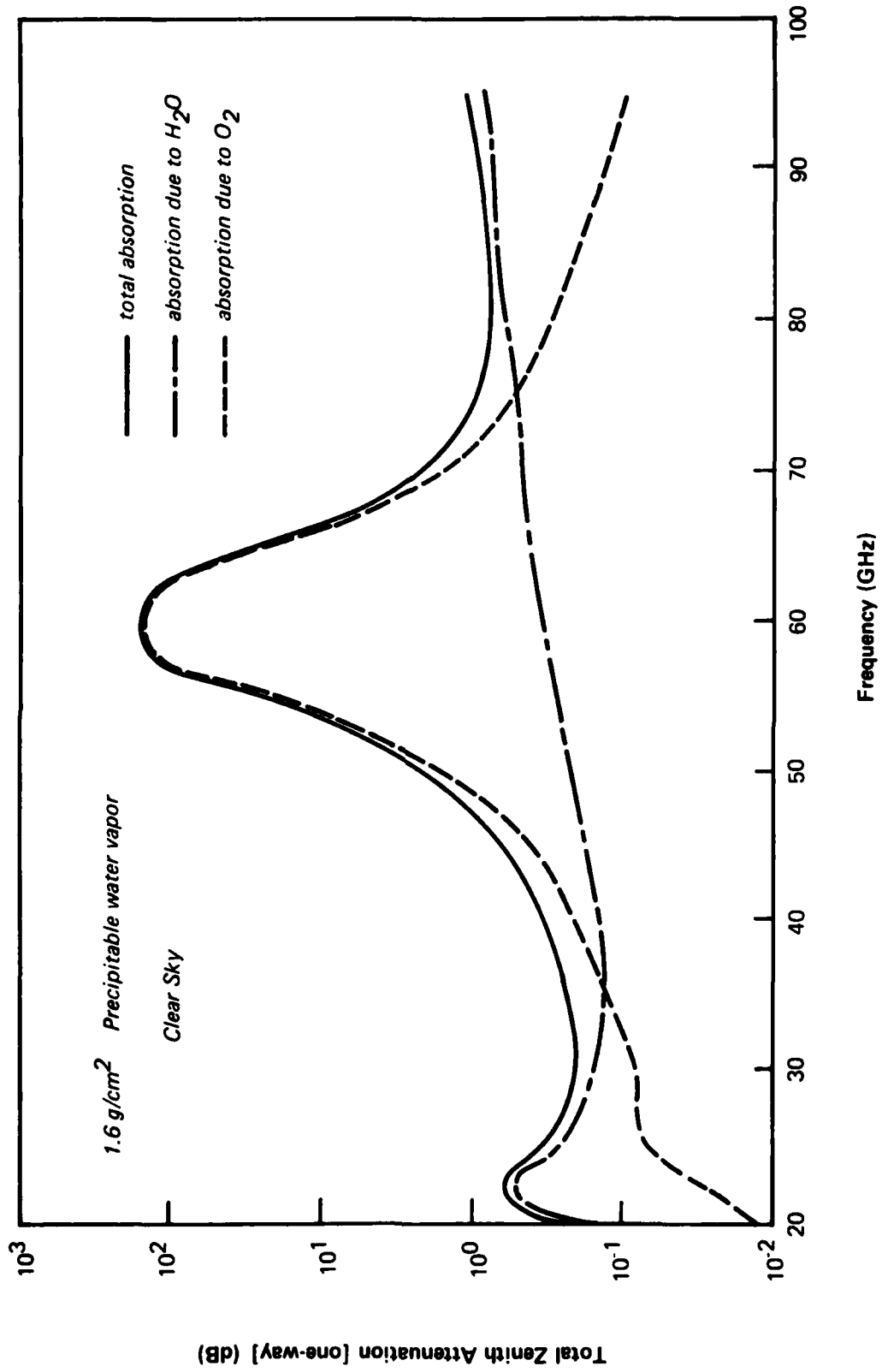


Figure 23 Zenith Attenuation vs Frequency for Atmospheric Gases

REFERENCES

- Atlas, D. (1964): "Advances in Radar Meteorology", in Advances in Geophysics, Vol. 10, pp. 317-478, Academic Press.
- Crane, R.K. (1966): "Microwave scattering parameters for New England rain", MIT Lincoln Laboratory Tech. Rept. 426.
- Crane, R.K. (1971): "Propagation phenomena affecting satellite communication systems operating in the centimeter and millimeter wavelength bands", Proc. IEEE, 59, 173-188.
- Crane, R.K. (1973): "Virginia precipitation experiment - data analyses", NASA/GSFC Doc. X-750-73-55, NASA Goddard Space Flight Center, Greenbelt, Maryland.
- Crane, R.K. (1974): "The rain range experiment - propagation through a simulated rain environment", IEEE Trans. Antennas and Propagat., AP-22, 321-328.
- Crane, R.K. (1975): "Attenuation due to rain - a mini review", IEEE Trans. Antennas and Propagat., AP-23, 750-752.
- Crane, R.K. (1977): "Prediction of the effects of rain on satellite communication systems", Proc. IEEE, 63, 456-474.
- Crane, R.K. and J.M. Glover (1978): "Calibration of the SPANDAR radar at Wallops Island", Preprints 18th Conf. on Radar Meteorology.
- Currie, N.C., F.B. Dyer and R.D. Hayes (1975): "Analysis of radar rain return at frequencies of 9.375, 35, 70 and 95 GHz", EES/GIT Project A-1485 Tech. Rept. 2, Engineering Experiment Station, Georgia Institute of Technology.
- deBettencourt, J.T. (1974): "Statistics of millimeter-wave rainfall attenuation", J. Rech. Atmos., 8, 89-119.
- Joss, J., R. Cavalli and R.K. Crane (1974): "Good agreement between theory and experiment for attenuation data", J. Rech. Atmos., 8, 299-318.
- Laws, J.O. and D.A. Parsons (1974): "The relation of raindrop-size to intensity", Amer. Geophys. Union Trans., 24, 452-460.
- Marshall, J.S. and W. McK. Palmer (1948): "The distribution of raindrops with size", J. Meteorol., 5, 165-166.
- Medhurst, R.G. (1965): "Rainfall attenuation of centimeter waves: Comparison of theory and measurement", IEEE Trans. Antennas and Propagat., AP-13, 550-564.

REFERENCES (cont)

- Richard, V.W. and J.E. Kammerer (1975): "Rain backscatter measurements and theory at millimeter waves", BRL Rept. 1838, USA Ballistics Research Laboratories, Aberdeen Proving Ground, Maryland.
- Rosenkranz, P.W. (1975): "Shape of the 5 mm Oxygen Band in the atmosphere", IEEE Trans. Antennas and Propagat., 23, 498-506.
- Sander, J. (1975): "Rain attenuation of millimeter waves at $\lambda = 5.77$, 3.3 and 2 mm", IEEE Trans. Antennas and Propagat., AP-23, 213-220.
- Van Vleck, J.H. and V.F. Weisskopf (1945): "In the shape of collision-broadened lines", Rev. Mod. Phys., 17, 227-236.
- Waldteufel, P. (1973): "Attenuation des ondes hyperfréquences par la pluie: une mise au point", Ann. Telecommun., 28, 255-272.

UNCLASSIFIED

SECURITY CLASSIFICATION OF THIS PAGE (When Data Entered)

REPORT DOCUMENTATION PAGE		READ INSTRUCTIONS BEFORE COMPLETING FORM
1. REPORT NUMBER ESD/TR-80-84	2. GOVT ACCESSION NO. AD A088332	3. RECIPIENT'S CATALOG NUMBER
4. TITLE The Evaluation of Models for Atmospheric Attenuation and Backscatter Characteristic Estimation at 95 GHz.		5. TYPE OF REPORT & PERIOD COVERED Technical report
6. AUTHOR Robert K. Crane and Hsiao-hua K. / Burke		6. PERFORMING ORG. REPORT NUMBER ERT Document No. P-3606
7. PERFORMING ORGANIZATION NAME AND ADDRESS Environmental Research & Technology, Inc., Concord, MA 01742, under Purchase Order AX 14398 to M.I.T. Lincoln Laboratory		8. CONTRACT OR GRANT NUMBER(S) F19628-78-C-0002
9. CONTROLLING OFFICE NAME AND ADDRESS Air Force Systems Command, USAF Andrews AFB Washington, DC 20331		10. PROGRAM ELEMENT, PROJECT, TASK AREA & WORK UNIT NUMBERS
14. MONITORING AGENCY NAME & ADDRESS (if different from Controlling Office) Electronic Systems Division Hanscom AFB Bedford, MA 01731		12. REPORT DATE February 1978
16. DISTRIBUTION STATEMENT (of this Report) Approved for public release; distribution unlimited.		13. NUMBER OF PAGES 35
17. DISTRIBUTION STATEMENT (of the abstract entered in Block 20, if different from Report)		15. SECURITY CLASS. (of this report) UNCLASSIFIED
18. SUPPLEMENTARY NOTES None		15a. DECLASSIFICATION DOWNGRADING SCHEDULE
19. KEY WORDS (Continue on reverse side if necessary and identify by block number) 95 GHz propagation backscatter weather attenuation theoretical experimental data		
20. ABSTRACT (Continue on reverse side if necessary and identify by block number) A literature survey has been conducted and an analysis of the data made to determine which models for atmospheric attenuation and backscatter estimation at 95 GHz best applies. It is concluded that existing experimental data properly interpreted agree well with theoretical predictions.		

207650

LM